Applied Catalysis B: Environmental 219 (2017) 538–549

Contents lists available at ScienceDirect

Applied Catalysis B: Environmental

journal homepage: www.elsevier.com/locate/apcatb

A green solar photo-Fenton process for the elimination of bacteria and micropollutants in municipal wastewater treatment using mineral iron and natural organic acids

Paola Villegas- Guzman[a,b], Stefanos Giannakis[b], Sami Rtimi[b], Dominique Grandjean[c], Michaël Bensimon[c], Luiz Felippe de Alencastro[c], Ricardo Torres-Palma[a,*], César Pulgarin[b,*]

[a] Grupo de Investigación en Remediación Ambiental y Biocatálisis (GIRAB), Instituto de Química, Facultad de Ciencias Exactas y Naturales, Universidad de Antioquía UdeA, Calle 70 No. 52-21, Medellín, Colombia
[b] Ecole Polytechnique Fédérale de Lausanne, EPFL-SB-ISIC-GPAO, Station 6, CH-1015, Lausanne, Switzerland
[c] Ecole Polytechnique Fédérale de Lausanne, EPFL-GR-CEL, Station 2, CH-1015, Lausanne, Switzerland

ARTICLE INFO

Article history:
Received 20 May 2017
Received in revised form 20 July 2017
Accepted 24 July 2017
Available online 25 July 2017

Keywords:
Natural iron source
Near-neutral solar photo-Fenton
Iron organo-complex
Municipal wastewater treatment
Microorganisms
Micropollutants

ABSTRACT

In this investigation, a new, green photo-Fenton process for wastewater treatment is proposed, involving the use of a natural iron source and natural additives, deriving from wastes, acting as iron chelators. The use of mineral iron as precursor in the photo-Fenton process, instead of iron salts, was still able to promote *E. coli* inactivation. Furthermore, the addition of four low weight organic acids (citric, tartaric, ascorbic and caffeic) showed a significant enhancement of the process, reaching total inactivation except for caffeic acid, which showed no significant effects. Two natural products, rich in the promising organic acids were tested as additives, lime and orange juice, plus their infusion. Lime-based additives showed better results compared to orange-based ones, which could be attributed to the excessive addition of organic matter in the orange systems. The formation of photoactive complexes with the mineral iron and the organic acids from the natural products induced the production of reactive species and ferrous ion, sustaining a homogeneous Fenton reaction. Finally, the proposed modified process was tested against different secondary effluents from a municipal wastewater treatment plant. Total bacterial inactivation was reached in the lime-based system, with no visible microorganism regrowth after 48 h. Additionally, the process was able to eliminate 40% of the total identified micropollutants of the secondary effluent reaching almost 50% of removal of the total effluent organic matter.

1. Introduction

Over the last years, the photo-Fenton process became one of the most interesting alternative process for wastewater treatment, given its simplicity and feasible application [1–5]. Based on the photo-activity of the ferric species, this process can be considered catalytic, and an enhanced form of the classic Fenton reaction inducing the formation of extra hydroxyl radicals (Eqs. (1) and (2)). However, due to the insolubility of the ferric aquo or hydroxy species, the system is pH-dependent and its full scale application is subject to limitations [6,7]. Consequently, up to date, many investigations deal with the possibility to perform the photo-Fenton process at near-neutral pH [8]. Based on previous reports, the pH dependence can be minimized by the formation of ferric organo-complexes [9–11]. The substitution of aquo or hydroxyl groups for organic molecules as ligands involves the following facts: (i) the increment of dissolved iron at near-neutral pH [12]; (ii) the use of sunlight, as light radiation to induce the photochemistry of the complexes [2,13]; (iii) the formation of ferrous ion (Eq. (3)) [7,14,15], which promotes the classical Fenton reaction; (iv) the production of organic radicals that could contribute in the organic matter oxidation or produce extra transients (Eqs. (3) and (4)).

$$Fe^{2+} + H_2O_2 \rightarrow Fe^{3+} + OH^- + HO^\bullet \quad (1)$$

$$Fe(H_2O)_5(OH)^{2+} + h\nu \rightarrow Fe^{2+} + HO^\bullet \quad (2)$$

$$[Fe(RCOO)]^{2+} + h\nu \rightarrow Fe^{2+} + R^\bullet + CO_2 \quad (3)$$

* Corresponding authors.
E-mail addresses: ricardo.torres@udea.edu.co (R. Torres-Palma), Cesar.Pulgarin@epfl.ch (C. Pulgarin).

http://dx.doi.org/10.1016/j.apcatb.2017.07.066
0926-3373/

$$R^{\bullet} + O_2 \rightarrow\rightarrow O_2^{\bullet -} + CO_2 \quad (4)$$

Different organic compounds have been tested as effective ligands for ferric complexes, leading to an improved photo-Fenton process [10,16,17]. Among the organic compounds, carboxylic acids and phenols have been highlighted given their high chelating effect [7,18]. In fact, a previous investigation showed that the use of solar photo-Fenton for bacterial inactivation in wastewater was greatly enhanced by the addition organic acids such as citric, tartaric, ascorbic and caffeic acid [19]. This investigation evidenced the opportunity to improve the solar photo-Fenton efficiency against bacterial inactivation during wastewater treatment using natural products rich on the above-mentioned acids.

Besides the enhancement of the photo-Fenton process for wastewater treatment using natural products and solar radiation, another important factor worthy of consideration is the iron source. Up to date, different iron materials have been tested as precursors of the photo-Fenton process, including natural iron oxide [20], residue-based iron [21], zero valent metallic iron [22], magnetic composites [23] or modified clays and carbon-based materials [24] to promote organic pollutant degradation. However, among the iron species, a special attention is associated to the ferric ion, given that in natural conditions, Fe^{2+} is oxidize to Fe^{3+} by oxygen or H_2O_2, increasing the investigative interest for ferric sources. The use of natural iron materials has extra advantages associated to the stability of the material against light radiation, oxidation by dissolved oxygen and pH variation [25]. In addition, the presence of ferric ion in the system involves additional reactions (Eqs. (5)–(7)), in which extra oxidative species, such as superoxide radical ($HO_2^{\bullet}$), are produced.

$$Fe^{3+} + H_2O_2 \rightarrow Fe^{2+} + H^+ + HO_2^{\bullet} \quad (5)$$

$$Fe^{3+} + H_2O_2 \rightarrow Fe(OOH)^{2+} + H^+ \quad (6)$$

$$Fe(OOH)^{2+} \rightarrow HO_2^{\bullet} + Fe^{2+} \quad (7)$$

However, the existing literature on photo-Fenton treatment of WW is currently limited to studies where wastewater treatment is focused on either chemical [11] or microbiological contamination [3]. Moreover, the investigations with alternative iron materials are usually carried out in distilled water [22,20,21], which provide important information on alternative ferric sources but on the other hand, are far from a possible real application. Therefore, the aim of this investigation is to evaluate the use of a natural iron material as precursor of the photo-Fenton process, in order to promote the bacterial inactivation and micropollutants degradation of real secondary effluents. Additionally, the effects of the addition of natural products is sought, such as lime, orange juice and infusion, and valorizing alimentary and agricultural wastes, or turning the process into a greener alternative is also investigated.

2. Materials and methods

2.1. Reagents

Hydrogen peroxide 30%, citric acid ≥99.5%, L- ascobic acid ≥99.0%, L-(+)-tartaric acid ≥99.5%, caffeic acid ≥98.0%, acetate buffer solution pH 4.65, ferrozine 97% and hydroxylamine hydrochloride 99% were purchased by Sigma Aldrich. Titanium oxysulfate was supplied by Fluka; chloride acid, sulfuric acid and sodium hydroxide were supplied by Merck.

Preliminary experiments were carried out using simulated municipal secondary effluent reported by Muthukumaran et al. [26] and real effluents from the municipal wastewater treatment plant Vidy (Lausanne, Switzerland) previously treated by activated sludge or coagulation/flocculation process. The simulated wastewater characteristics are 39 ppm of chemical oxygen demand (COD), 9.8 ppm of dissolved organic carbon (DOC) and pH 7.5. The real wastewaters characteristics are presented in SM 1. Concerning the preliminary investigations, *E. coli* K-12 strain (MG 1655) was provided from "Deutsche Sammlung von Mikroorganismen und Zellkulturen". The working bacteria solution was prepared as previously reported [27] obtaining a 10^9 CFU/mL initial concentration. The real WW experiments deal with the indigenous population of the matrix as described in Giannakis et al. [6].

2.2. Iron material

As iron source, a natural material from an iron mine of Colombia (Duitama, Boyacá) was used without pretreatment. The specific surface area was estimated in 19.79 m^2/g by the Brunauer–Emmett–Teller (BET) theory, and N_2 physisorption measurements on a Micromeritics 3Flex apparatus was used for its measurement. Analyses took place at liquid nitrogen temperature, and between 10^{-5} and 0.99 relative N_2 pressure. Around 150 mg sample was dried for 4 h at 120 °C (2 °C/min) under vacuum (<10^{-3} mbar) and a leak test was assayed before analysis. For the high-resolution TEM, FEI Osiris was used and operated in 200 kV, with Spot size of 5, dwell time 50 μs, real time 600s. Fig. 1 shows the grain size and distribution of the elements. EDX mapping was acquired using Esprit software and shown in supplementary material (SM 2). An XRF analysis using a pellet of the material (area 1.8 × 2.3 cm2, spot size 30 μm, 1000 ms dwell time, Matrix 128 × 100; duration 5.1 h) and a mapping showed 81.26% of iron content (SM 3). The crystallographic phases were determined by X-ray diffraction (XRD) using Cu Kα radiation at a grazing incident angle of 4° (X'Pert MPD PRO from PANalytical). The sample was sieved to separate big aggregates (to avoid x-ray reflection due to size), suspended in MQ-water then dropped/fixed on glass slide. The XRD pattern of the natural iron is presented in SM 4 of the Supplementary material.

2.3. Process description

A lab scale Suntest solar simulator (Hanau) equipped with an air-cooled Xenon lamp 1500-W, with illumination surface of 560 cm^2 and 600 W/m^2 of solar intensity (global irradiance) was used to perform the solar photo-Fenton experiments. The emitted radiation is characterized as follows: 0.5% of UVB (290–320 nm) and 5–7% of UVA (320–400 nm), while after 400 nm the solar spectrum is simulated. Finally, UVC and IR wavelengths were filtered by an uncoated quartz glass light tube and cut-off filters, respectively.

Bacterial inactivation tests were carried out in Pyrex glass bottle reactors, using constant stirring at 400 rpm. In absence of light, 100 mL of wastewater (for both experiments in synthetic and real WW) was mixed during 10 min with the tested additives, followed by the addition of 500 μL of the iron material suspension (100 μg/10 mL) and a subsequent mixing for 10 min 100 μL of *E. coli* of working bacteria solution was added in the reactor (sample t = 0 min, bacterial concentration: 10^6 CFU/mL). After 10 min of stirring, hydrogen peroxide was added into the system (25 ppm in the reactor) and the sunlight simulator is turned on. Aliquots of 1000 μL from the bulk of the solution were sampled at pre-determined time points, and each experiment was performed at least in duplicate.

2.4. Natural products extractions

Natural products were tested as additives using commercially available fruits: orange (*citrus tangelo*) and lime (*citrus lime*). Juice and aqueous extraction (infusion) from the peels of both fruits were tested, as described in Villegas-Guzman et al. [19]. The juice was separated from the peel by handle squeezing. The peels were grinded after drying at 60 °C for 24 h followed by an aqueous

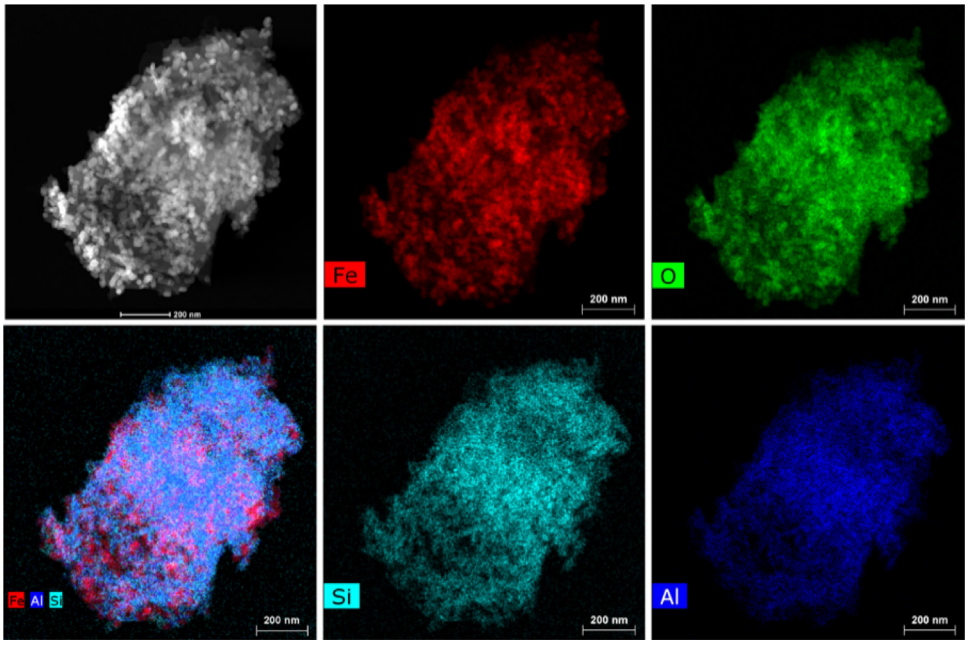

Fig. 1. HR-TEM image of the natural iron material.

infusion: 2 g of dried material was mixed with 40 mL of boiling water for 5 min. The mixture was then centrifuged for 5 min at 5000 rpm. All the natural products (juices and extractions) used along the investigation were freshly obtained and immediately used for experiments.

2.5. Analytical measurements during experiments

2.5.1. Bacterial enumeration

Bacterial quantification was performed by the spread plate method as reported by Giannakis et al. [28]. Two consecutive dilutions were plated in duplicate for each sample point obtaining less than 7% of difference (max. error measured in this study), therefore the standard deviation is not plotted for simplicity of the graphs.

2.5.2. Iron and hydrogen peroxide quantification

The total dissolved iron along the experiments was quantified using the ferrozine method [14] and the hydrogen peroxide concentration was determined by the titanium oxysulfate method [29]. Absorbance of the samples was determined using a UV-1800 spectrophotometer (Shimadzu, Japan). Experiments were performed at least in duplicate and less than 5% of difference was obtained.

2.5.3. COD and DOC determination

The chemical oxygen demand (COD) analysis was performed by the closed reflux method using a digestion reactor with low and high range vials, acquired from HACH and a HACH Lange GmbH DR/3900 spectrophotometer. The dissolved organic carbon (DOC) was monitored by catalytic oxidation/NDIR combustion (TOC-VCS/N standard model) using a SHIMADZU TOC 500 equipped with an ASI auto-sampler (Schweiz GmbH, Reinach, Switzerland), with 0.45 μm pore size filtering of the real WW samples prior to analysis.

2.5.4. Micropollutants monitoring and evaluation

An online solid phase extraction (SPE) method followed by UPLC/MS-MS, with a capability of simultaneous measurement of 28 micropollutants was developed and used in this study. The specifications of the micropollutants (MW, LOD and LOQ) can be found in Table 1. For details on the conditions, interested readers can refer to De la Cruz et al. [15] and Giannakis et al. [30]. Out of the 28 MPs available in the developed method, 21 were monitored effectively and their degradation was followed before and after the variations of the photo Fenton treatment.

3. Results and discussion

3.1. Solar photo-Fenton process using a natural iron source

In order to evaluate the possible application of a natural iron material (M-Fe) as alternative reactant for the solar photo-Fenton process, experiments of *E. coli* inactivation using simulated wastewater were performed (Fig. 2). Based in the results, the use of this material in the system alongside with H_2O_2, is able to inactivate 2 log CFU/mL, after 180 min of treatment. The observed efficiency could be attributed to the following pathways:

- A heterogeneous photo-Fenton process takes place, in which different ROS are produced [31] responsible of inducing bacterial inactivation. The two main pathways are the semiconductor mode of action of the natural iron oxides, or their participation as iron precursors. However, since in this set of experiments we cannot exclude or demonstrate the separate effect of the two actions, we suggest that *E. coli* inactivation is most probably taking place by the latter process, which can generate $HO^{\bullet}$, possessing higher inactivation capabilities, and disinfection does not strictly rely on the oxidative action of the holes (h^+).
- A homogeneous Fenton process led by the leached iron and the added hydrogen peroxide is inducing bacterial inactivation. In order to evaluate the contribution of the homogeneous Fenton reaction, dissolved iron and hydrogen peroxide consumption were determined throughout the test (Fig. 3). According to the results, less than 0.1 ppm of iron is leached into the bulk during the treatment for the M-Fe/H_2O_2 system. Moreover, the evolution of H_2O_2 shows a considerable consumption of hydrogen peroxide indicating an important participation of this in the process. However, a control experiment (SM 5) shows no significant reduction in the bacteria counting by the H_2O_2/solar system. As a consequence, the contribution of the hydrogen peroxide oxidative action and the effect of sunlight radiation in the solar

Table 1
Micropollutants identification in the secondary effluent after activated sludge.

	Category	Specification	MW (g/mol)	LOQ (ng/L)	Detected concentration (ng/L)
Atenolol	Drug	β-blocker	266.336	5	727 ± 50
Atrazine	Chemical	Pesticide	215.68	2	4.91 ± 0.29
Benzotriazole	Chemical	Corrosion Inhibitor	119.13	15	2889 ± 437
Bezafibrate	Drug	Lipid regulator	361.819	2	458 ± 59
Carbamazepine	Drug	Anti-epileptic	236.269	2	164 ± 20
Clarithromycin	Drug	Antibiotic	747.953	2	515 ± 59
Diclofenac	Drug	NSAID	296.148	5	1364 ± 196
Diuron	Chemical	Herbicide	233.1	5	12.1 ± 3.6
Gabapentin	Drug	Anti-epileptic	171.237	2	1467 ± 370
Iomeprol	Drug	ICM	777.09	50	8118 ± 1430
Irgarol	Chemical	Pesticide	253.367		ND
Isoproturon	Chemical	Herbicide	206.284		ND
Ketoprofen	Drug	NSAID	254.281		NR
Mecoprop	Chemical	Herbicide	214.646	5	13.8 ± 3.1
Methylbenzotriazole	Chemical	Corrosion Inhibitor	133.51	2	752 ± 122
Metolachlor	Chemical	Herbicide	283.8		ND
Metoprolol	Drug	β-blocker	267.364	2	374 ± 61
Metronidazole	Drug	Antibiotic	171.15	5	1773 ± 250
Naproxen	Drug	NSAID	230.259	15	1190 ± 149
Norfloxacin	Drug	Antibiotic	319.331		ND
Ofloxacin	Drug	Antibiotic	361.368	2	91.6 ± 10.2
Paracetamol	Drug	Pain-reliever	151.163		NR
Primidone	Drug	Anticonvulsant	218.252	5	60.5 ± 9.8
Simvastatin	Drug	Lipid regulator	418.566		ND
Sulfamethoxazole	Drug	Antibiotic	253.279	10	498 ± 73
Terbutryn	Chemical	Herbicide	241.356	2	8.8 ± 1.3
Trimethoprim	Drug	Antibiotic	290.32	2	179 ± 23
Venlafaxine	Drug	Anti-depressive	277.402	2	187 ± 27

NR: not readable; ND: not detected.

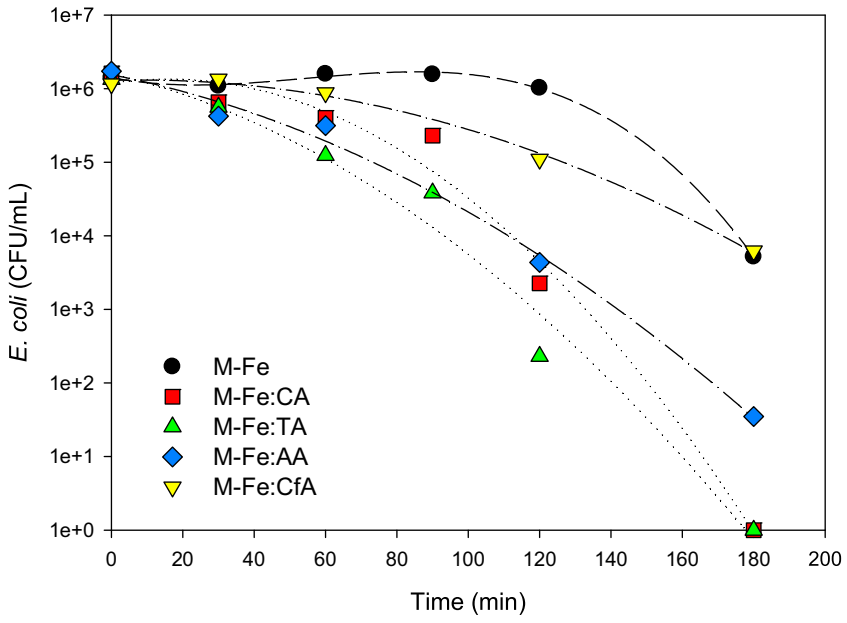

Fig. 2. *E. coli* inactivation by solar photo-Fenton using the sole iron material (M-Fe) and iron material with organic acids (1:0.5): citric acid (M-Fe:CA); tartaric acid (M-Fe:TA); ascorbic acid (M-Fe:AA) and caffeic acid (M-Fe:CfA). [M-Fe] = 5 ppm; [H_2O_2] = 25 ppm; 600 W/m^2.

photo-Fenton process using a natural material of iron is low, and targets non-selectively the organic matter in the bulk and the microorganisms present. Hence, the results suggest that this small amount of dissolved iron could be enough to promote a homogeneous Fenton reaction.

A notable fact is that a partial inactivation of *E. coli* is only observed after 120 min of treatment when the mineral iron material (M-Fe) is used. In WW, high competition of the dissolved organic matter from the wastewater for the few produced hydroxyl radicals takes place. Consequently, the solar photo-Fenton process using the natural iron material source is limited by the amount of leached iron from the material to induce the homogeneous Fenton reaction, and is most probably led by the heterogeneous process.

As the solubilization and photo-dissolution of iron from the mineral source is limited, the addition of agents that could increase the amount of iron in the bulk was challenged. Low weight organic acids are known to efficiently act as iron ligands, and hence could allow the photo-Fenton process to be carried out at near-neutral pH. In the previous M-Fe system, four organic acids were added, commonly found in natural products or agricultural and alimentary wastes, and were tested in their potential enhancement of the

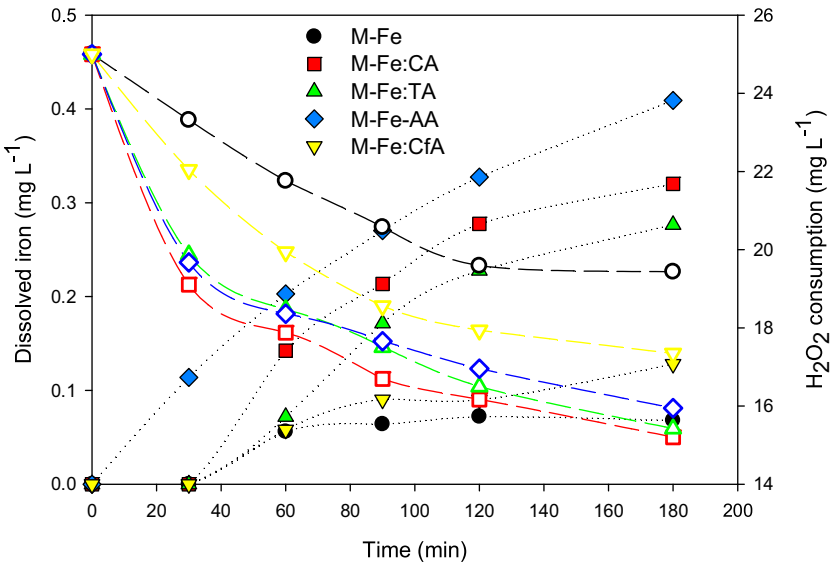

Fig. 3. Dissolved iron evolution (fill symbols) and hydrogen peroxide (open symbols) consumption during *E. coli* inactivation by solar photo-Fenton using the sole iron material (M-Fe) and iron material with organic acids (1:0.5): citric acid (M-Fe:CA); tartaric acid (M-Fe:TA); ascorbic acid (M-Fe:AA) and caffeic acid (M-Fe:CfA). [M-Fe] = 5 ppm; [H_2O_2] = 25 ppm; 600 W/m^2.

photo-Fenton process (Fig. 2): citric acid (CA), tartaric acid (TA), ascorbic acid (AA) and caffeic acid (CfA). The amount of iron: organic acid (OA) added into the system was fixed at a 1:0.5 molar ratio M-Fe:OA. After addition, the lowest pH was observed in CA (pH 5), which was considered safe in terms avoiding bacterial inactivation by the matrix conditions, or over-acidifying the WW. Fig. 2 shows that the presence of the acids, except the caffeic acid, significantly enhance the process, reaching total inactivation for CA and TA, followed by AA (almost 5-log reduction). These enhancements can be explained by the amount of dissolved iron in the system and H_2O_2 consumption during the process. In all cases, iron in the bulk was higher when CA, TA and AA were added compared to the sole M-Fe system and the one with caffeic acid (M-Fe:CfA) (Fig. 3).

The increment of iron in the presence of organic acids can be attributed to different factors regarding structural and chemical properties of the acids. The action of CA, TA and AA during the solar photo-Fenton process has been previously reported leading to several factors that enhance the *E. coli* inactivation, when $FeSO_4$ and $Fe_2(SO_4)_3$ were used as iron sources [19].

Concerning these specific organic acids, certain conclusions can be drawn. Both CA and TA are able to enhance the production of hydroxyl radicals through the Fenton reaction, increasing the effectiveness of the process at near neutral pH to degrade microorganisms and micropollutants [12,16,29,32,33]. This positive effect is associated with:

a) The formation of soluble ferric complexes that enhance the homogeneous Fenton reaction, thus increasing the efficiency of the process. Here, we verify this observation by quantification of the dissolved iron; a significant increase along the treatment, after the addition of CA and TA was observed.

b) The formation of photo-active complexes. Although the quantity of iron photo-dissolved at the beginning is similar to the sole M-Fe addition (and is a function of the mineral), in presence of the organic ligands, photo-active complexes are generated, and undergo an efficient LMCT, reducing iron from Fe^{3+} to Fe^{2+} to participate again in the Fenton process and production of oxidized ligands, which initiate the production of further ROS.

On the other hand, AA has a major action as a reductive agent. Therefore, in the presence of AA, the iron recycling takes place more effectively (Eqs. (8)–(11)) and Fe^{3+} from the natural material is easily reduced to soluble Fe^{2+}, thus enhancing the Fenton reaction. The amount of dissolved iron in the presence of AA, which is the highest among the tested systems, verifies our hypothesis. Possibly, the iron reduction process could be further enhanced by increasing AA concentration. Additionally, it has been reported that the main reductive action of the AA is attributed to certain structures present due to its equilibrium, such as the ascorbate monoanion and dehydroascorbate anion [34]. As a result, the positive effect of AA in the system is pH dependent.

$$Fe^{3+} + AA \rightarrow Fe^{2+} + AA_{ox} \quad (8)$$

$$Fe^{2+} + O_2 \rightarrow O_2^{\bullet -} + Fe^{3+} \quad (9)$$

$$O_2^{\bullet -} + H^+ \rightarrow H_2O_2 \quad (10)$$

$$Fe^{2+} + H_2O_2 \rightarrow HO^{\bullet} \quad (11)$$

Finally, interestingly enough, the dissolved iron evolution by the addition of CfA is similar to the M-Fe system suggesting that, under the chosen experimental conditions, CfA does not act as an efficient ligand and promote the complexation of iron in the solution. However, the H_2O_2 consumption in this case is much higher than M-Fe system. This effect could be attributed to the reductive character of the CfA [35] and the direct reaction between H_2O_2 and CfA which could be taking place. A similar finding is also observed for M-Fe:AA system, where H_2O_2 consumption is the highest despite that *E. coli* inactivation is not as efficient as M-Fe:CA or M-Fe:TA. Hence, the ligands that act as reductive agents consume more H_2O_2, depriving its efficient allocation in the production of ROS which may lead to bacterial inactivation. Also, we note that since near-neutral pH values were chosen as starting conditions, optimization of the CfA and AA addition was not performed, to verify the boundary conditions and possible experimental space where CfA and AA could act beneficially.

3.2. E. coli *inactivation by solar photo-Fenton using natural products*

Considering the beneficial use of organic acids, such as the citric, tartaric and ascorbic acid as enhancements of *E. coli* inactivation in wastewater using a natural iron source, natural products containing these acids were tested under the same scope. In a previous work, we demonstrated that the addition of natural products, rich

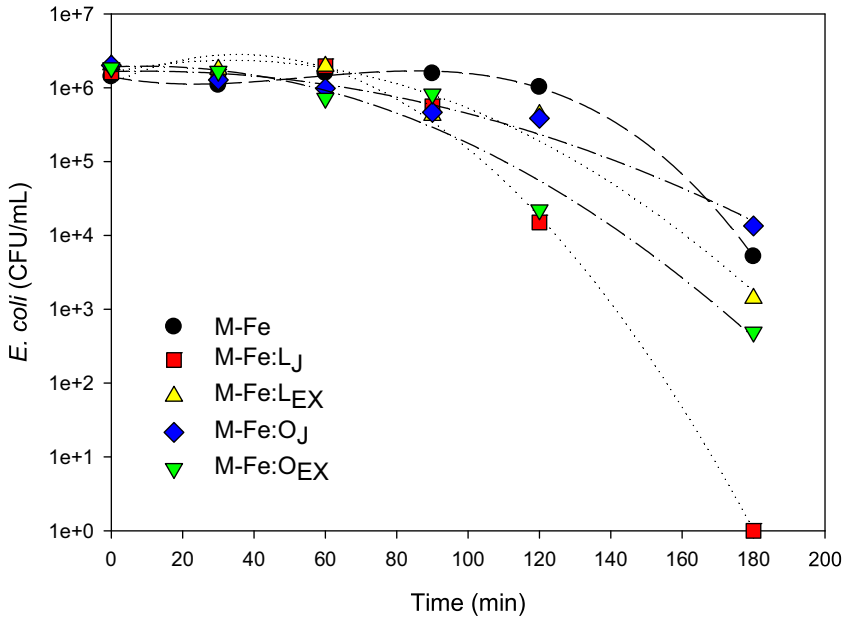

Fig. 4. *E. coli* inactivation by solar photo-Fenton using a natural material of iron (M-Fe) and natural products: lime juice (L_J) and aqueous extraction (L_{EX}); orange juice (O_J) and aqueous extraction (O_{EX}). [M- Fe] = 5 ppm; [H_2O_2] = 25 ppm; 600 W/m^2. (For interpretation of the references to colour in this figure legend, the reader is referred to the web version of this article.)

in these acids can enhance *E. coli* inactivation in a homogeneous Fenton system [19] if iron salts are used as iron precursors. As a consequence, it is interesting to evaluate the effect of fruits, such as lime (L) and orange (O) in a heterogeneous system for wastewater disinfection by solar photo-Fenton using a natural iron material, and variants of the fruit products.

The evaluation of natural products was determined by the addition of the juice (J) and an aqueous extraction (EX) form the fruits peel (infusion method, see Materials and Methods section). In the following experiments, the addition of the natural products amount was controlled by the final pH of the WW, resulting from their addition in the bulk, since a mixture of the aforementioned acids governs these solutions; for comparison reasons, the pH of the solution after the addition of the juice/infusion was set at 6. Fig. 4 shows the bacterial inactivation when natural products were added in the system and compared to the system without additives (M-Fe). Interestingly, there is no apparent inhibition by the organic matter added in the matrix when the natural products were introduced into the systems. In fact, a significant enhancement of bacterial inactivation was observed in the M-Fe:L_J system followed by the M- Fe:O_{EX} system. The H_2O_2 consumption was measured along the treatment showing no significant difference between all the tested systems (SM 6). The major enhancement of L_J could be associated to the composition of the lime juice, which contains high amounts of citric acid, but also tartaric and ascorbic acid as main constituents [36] . These findings suggest that, under the selected experimental conditions, the CA, TA and AA of the lime juice are able to: i) efficiently produce ferric complexes with the iron material, that lead to the reactive species formation and increase the amount of iron in the solution; these complexes could then fuel a homogeneous Fenton reaction to end up into hydroxyl radicals also responsible of E. coli inactivation, or ii) generate photo-active complexes, facilitating the LMCT presented before.

However, aqueous extractions from both lime and orange fruit peel, as well as the orange juice, are also rich in the aforementioned acids. In order to have deep understanding of the different effects, the initial organic carbon was determined for each system (Table 2). It can be noticed that the addition of both lime juice (L_J) and extraction (L_{EX}) did not have a significant impact on the TOC, compared to the addition of the orange-based products (O_J and O_{EX}). As a result, the positive effect of the lime juice could be attributed to the molar ratio between the contained CA, TA and AA in the samples and the organic matter of the matrix. Based on the fruits composition [37–39], this molar ratio is probably higher for lime than the orange fruit. Consequently, the negative effect of the extra organic matter from the added product is surpassed in the lime system by the positive effect of the organic acids. As this effect is only noticed in the M-Fe:L_J system and not in the M-Fe:L_{EX}, the aqueous extraction from the peel probably has a low molar ratio between the extracted organic acids and the rest of the soluble organic matter. Orange-based products on the other hand, present a higher increase in organic matter. Hence, higher competition for the generated ROS is taking place, and the enhancement of bacterial inactivation is moderate.

Table 2
Initial total organic carbon for the wastewater (WW) and the addition of lime juice (WW + L_J), lime aqueous extraction (WW + L_{EX}), orange juice (WW + O_J) and orange aqueous extraction (WW + O_{EX}).

	WW	WW + L_J	WW + L_{EX}	WW + O_J	WW + O_{EX}
TOC_0 (mg L^{-1})	9.2	18.2	11.5	191.2	100.6

3.3. Microorganisms and micropollutants elimination in activated sludge and coagulation- flocculation effluents using the modified solar photo-Fenton process

3.3.1. Total heterotrophic bacteria inactivation and regrowth

The promising results of the natural products to promote wastewater disinfection using a natural source of iron allows to investigate a green way to perform the solar photo-Fenton in real WW effluents. Fig. 5 shows the effect of the pure organic acids (Fig. 5A) and the natural products (Fig. 5B) compared to the system without additions using municipal wastewaters pretreated by activated sludge.

The sole M-Fe system (without acids) was able to induce *E. coli* inactivation after 270 min of treatment. Wastewaters are highly concentrated of dissolved organic matter, which are known to be

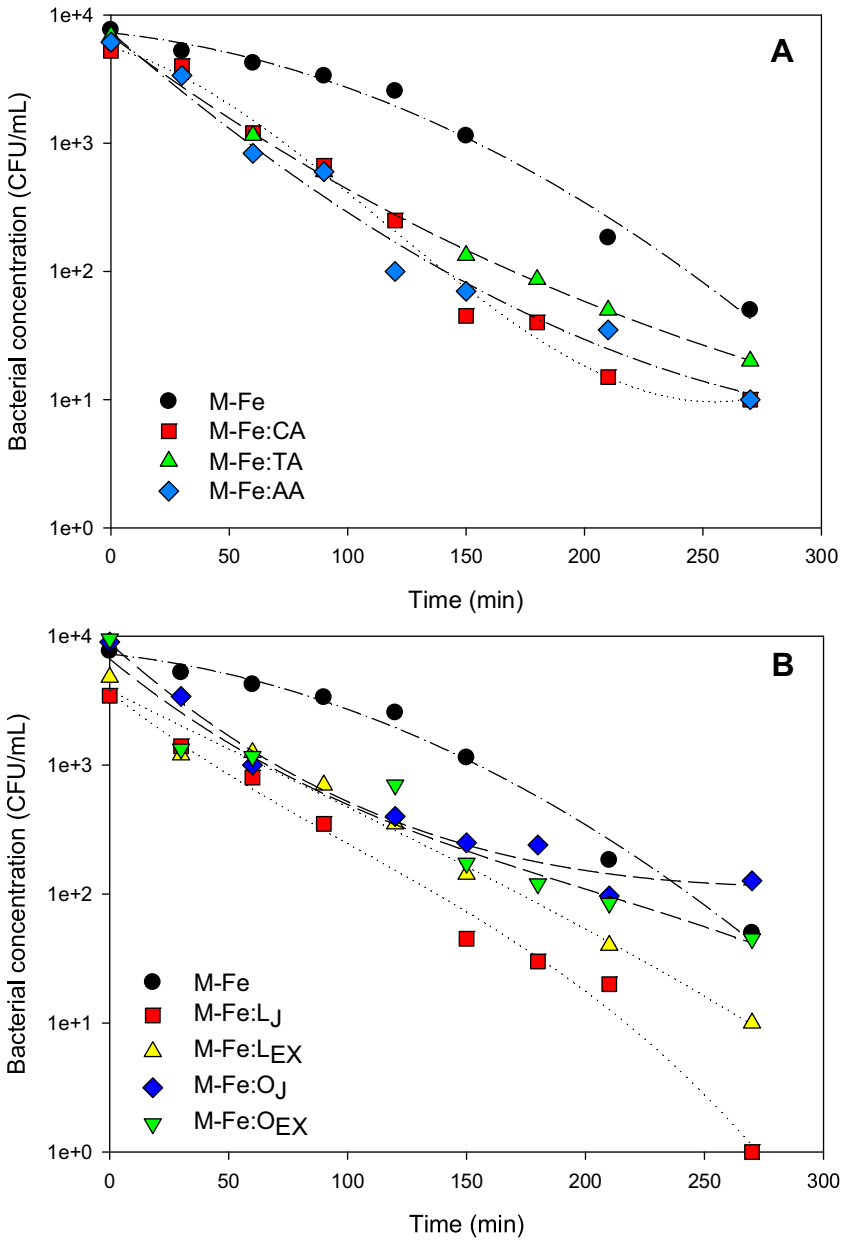

Fig. 5. Total bacterial detected by spread plate and PCA agar in secondary effluents treated by solar photo-Fenton using a natural iron material (M-Fe) in the presence of (A) organic acids (1:0.5): citric acid (M-Fe:CA); tartaric acid (M-Fe:TA); ascorbic acid (M-Fe:AA) and caffeic acid (M-Fe:CfA); (B) natural products: lime juice (L_J) and aqueous extraction (L_{EX}); orange juice (O_J) and aqueous extraction (O_{EX}). [M-Fe] = 5 ppm; [H_2O_2] = 25 ppm; 600 W/m^2. (For interpretation of the references to colour in this figure legend, the reader is referred to the web version of this article.)

efficient chelates of iron, as well containing ROS scavengers such as bicarbonates, which hamper the inactivation of microorganisms. However, given the dual action of the effluent organic matter (EfOM) [30], the presence of these compounds in the system allows the production of photoactive ferric complexes and the complexation of iron leached from the material to the bulk, leading to a homogeneous Fenton reaction.

A notable enhancement can be observed by the addition of all acids (CA, TA and AA) (Fig. 5A). This indicates that even in a very complex matrix such as the secondary effluent of municipal treatment plant, the effect of these acids as chelates for soluble photoactive ferric complexes or the direct reduction of Fe^{3+} to Fe^{2+}, is predominant.

The effect of natural products shows an enhanced process during 180 min of treatment (Fig. 5B). After this time, the orange-based systems presented slower kinetics. More promising results were observed for the lime-based systems where *E. coli* inactivation was effectively achieved. In fact, for the M-Fe:L_J no bacteria colonies were observed at the end of the treatment showing a promising and innovative way to enhance the solar photo-Fenton process for real wastewater disinfection.

On the other hand, according to the results, bacterial inactivation kinetics in the orange-based systems tended to decelerate after 180 min. During the process, both bacteria and dissolved organic matter are continuously consuming the produced hydroxyl radicals or other reactive species and the added acids acting as ligands or reductive agents, are also consumed. After 180 min of reaction, the positive effect of the organic acids is minimized by their absence in the medium. Additionally, given the complexity of the matrix (SM 1), both inorganic and organic species compete with the bacteria for the produced reactive species. Consequently, *E. coli* inactiva-

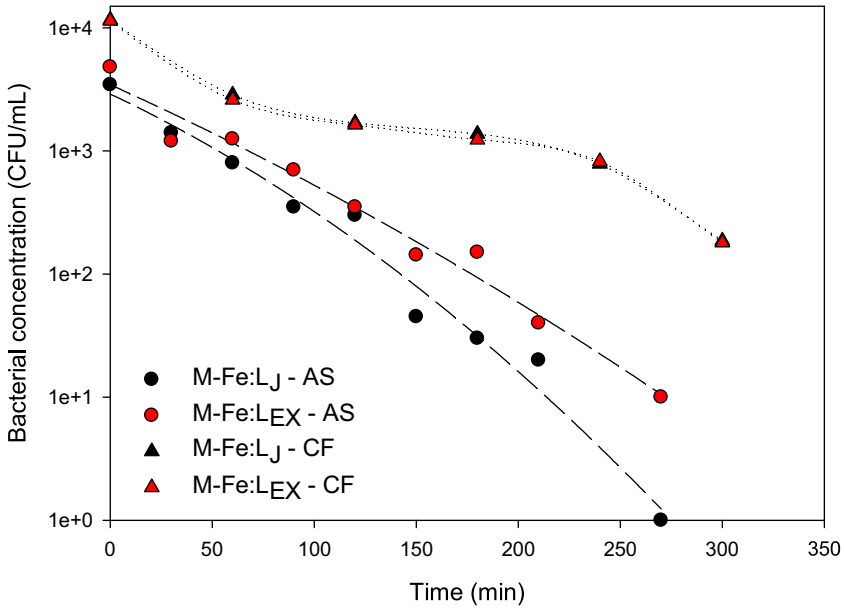

Fig. 6. Total bacterial detected by spread plate and PCA agar in secondary effluents treated by solar photo-Fenton solar photo-Fenton using a natural source of iron (M-Fe) in the presence of lime juice (L_J) and a lime aqueous extraction (L_{EX}). AS: activated sludge; CF: coagulation/flocculation. [M-Fe] = 5 ppm; [H_2O_2] = 25 ppm; 600 W/m^2.

tion is slower as the process evolves and the EfOM/Bacteria ratio increases.

A noteworthy milestone achieved by the modified photo-Fenton process is the elimination of bacterial regrowth. One would expect that the risk of leftover bacteria in a matrix spiked with readily assimilable organic matter, such as the juices and extracts would provide ground for efficient bacterial recovery. On the contrary, regrowth was evaluated for both systems with lime-based additives. No bacterial colonies were observed whatsoever, for 48 h after the treatment was concluded. We should also remind that in this part of the study, the whole consortium of heterotrophic microorganisms is accounted for, which includes more resistant microorganisms than the lab strain of *E. coli* K-12 previously used [3].

Considering the remarkable performance of the lime-based system using the natural iron material in activated sludge process effluents, we investigated the efficiency of this process after basic physicochemical treatment, commonly found in developing countries. For this purpose, *E. coli* inactivation was determined in waters after a coagulation/flocculation process, and comparison with the activated sludge effluents is presented in Fig. 6. A notable difference in the two families of kinetics can be observed, owing to the matrix characteristics. Wastewaters pre-treated by coagulation/flocculation (CF) showed an inhibition of bacterial inactivation compared to the ones treated by activated sludge (AS) process. A significant 2-log difference in inactivation is observed between CF and AS effluents, while among AS effluents, the lime juice was proven to perform better.

The reduced inactivation presented in CF effluents is due to the fact that CF effluents contain higher amounts of organics and solids (SM 1), hence higher ROS scavenging and less light penetration. More specifically, according to the wastewater characterization, CF effluents contain higher concentration of organic matter (TOC and DOC) than AS ones. More organic matter results to extra competition for the produced oxidative species by the M-Fe:Lime-based products in the modified photo- Fenton system, thus decreasing the process efficiency. Additionally, the total suspended solids (TSS) shows higher concentration of these in the coagulation/flocculation samples turning into an impediment for light radiation to reach the bulk. Consequently, the photocatalytic efficiency of the process is highly affected. This fact was verified by the lower UV_T of effluents from CF compared to those from AS (SM 1). Finally, it should be noted that CF is achieved by the addition of $FeCl_3$ in the bulk, and the residual effect is almost 10 times higher dissolved Fe concentration in the effluents, compared to AS. Hence, the addition of any organic acid acts beneficially, although it cannot compensate for the previous unfavorable facts.

3.3.2. *A process for developed countries: micropollutants degradation in AS effluents*

The addition of natural products has shown an enhanced bacterial inactivation in secondary effluents using the solar photo-Fenton process without prior pH modification. As the chronic risks related with the micropllutants (MP) content in wastewaters are amongst the hottest topics in environmental engineering, the assessment of this process for micropollutant degradation was effectuated. In the acquired samples we identified and followed the degradation of 21 drugs and chemical compounds, summarized by category and class in Table 1.

From the choice of the pollutants, a wide variation concerning structural properties and pharmacological action was selected. Therefore, in order to evaluate the process efficiency for organic pollutant elimination, the total micropollutants removal was determined and plotted (Fig. 7). The overall degradation of micropollutants was calculated by weighted arithmetic mean (Eq. (12)):

$$X(\%) = \frac{w_1 x_1 + \ldots w_{21} x_{21}}{w_1 + \ldots + w_{21}} \quad (12)$$

In Eq. (12), $X\%$ is the overall MP removal (in percentage), w_i is the quantity of the pollutant (in mol) and x_i the percentage of removal of each micropollutant. The results in Fig. 7 shows a significant elimination of the pollutants (in average ~35% of removal) after 6 h of treatment when the natural products were added into the system, while the sole iron material (M-Fe) reached only an average of ~17%. In detail, the results of the sole M-Fe photo-Fenton process vs. the enhanced versions can be found in Table 3. These results indicate the success of a process that was designed for bacterial inactivation, and in parallel achieves up higher removal of MPs, despite the extra added organic matter, up to 36.59%.

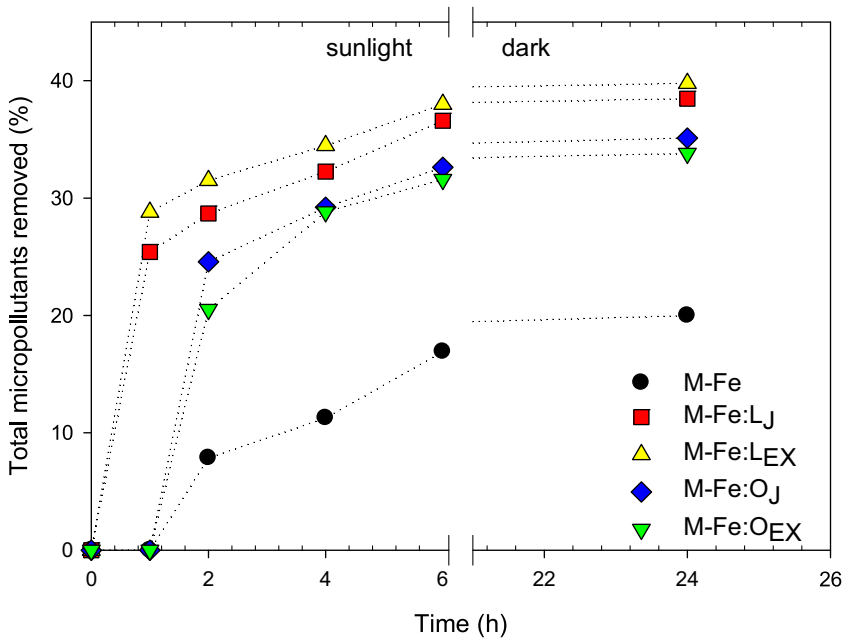

Fig. 7. Total micropollutant elimination during the secondary effluents treatment by solar photo-Fenton using a natural iron material (M-Fe) in the presence natural products: lime juice (L_J) and aqueous extraction (L_{EX}); orange juice (O_J) and aqueous extraction (O_{EX}). [M-Fe] = 5 ppm; [H_2O_2] = 25 ppm; 600 W/m^2. (For interpretation of the references to colour in this figure legend, the reader is referred to the web version of this article.)

Table 3
Degradation% of the detected micropollutants in activated sludge by various tested processes: sole M-Fe solar photo-Fenton (M-Fe spF) and the addition of lime juice (L_J), lime extraction (L_{EX}), orange juice (O_J) and orange extraction (O_{EX}).

	% degradation by the sole M-Fe spF	% degradation by M-Fe spF enhanced with L_J	% degradation by M-Fe spF enhanced with L_{EX}	% degradation by M-Fe spF enhanced with O_J	% degradation by M-Fe spF enhanced with O_{EX}
Atenolol	13.79	19.39	22.67	16.01	17.32
Atrazine	17.78	20.74	23.78	23.78	21.48
Benzotriazole	8.95	24.77	29.43	19.89	19.97
Bezafibrate	19.78	35.09	37.89	32.44	33.63
Carbamazepine	16.43	38.38	40.92	32.27	28.59
Clarithromycin	5.49	26.75	36.95	24.70	8.75
Diclofenac	73.57	80.59	78.14	66.38	67.49
Diuron	30	37.49	41.88	42.20	38.74
Gabapentin	6.48	29.16	26.34	25.07	27.24
Iomeprol	8.79	32.07	30.76	29.49	28.49
Mecoprop	1.72	42.19	36.99	36.16	31.78
Methyl-benzotriazole	5.96	19.85	25.76	12.84	15.31
Metoprolol	11.76	28.47	30.46	21.31	25.51
Metronidazole	72.6	74.65	73.72	68.01	72.30
Naproxen	73.76	80.39	83.21	72.97	75.23
Ofloxacin	73.38	77.73	78.24	65.99	70.65
Primidone	16.71	27.53	30.37	33.50	28.62
Sulfamethoxazole	25.29	63.64	30.33	41.73	26.44
Terbutryn	21.52	39.18	44.33	43.09	41.74
Trimethoprim	11.17	26.64	33.11	20.00	22.92
Venlafaxine	10.95	30.51	37.43	14.80	25.53
TOTAL	***16.91%***	***36.59%***	***35.99%***	***32.62%***	***31.58%***

More specifically, among the tested drugs, some patterns emerged, concerning the degradation profile of the different MPs. For instance, Methylbenzotriazole, Atenolol, Atrazine, Benzotriazole and Clarithromycin were the MPs with the lowest overall removal during a 6-h period, regardless of the enhancement, while Terbutryn, Metronidazole, Ofloxacin, Naproxen and Diclofenac were the most easily eliminated ones (bottom 5 and top 5 degraded, respectively). Concerning the enhancements, in increasing order of efficiency, the MP elimination was: Orange Infusion (31.58%) < Orange Juice (32.62%) < Lime Juice (35.99%) < Lime Infusion (36.59%). As the OJ and OI degradation rates are close, the results corroborate with the results acquired for the bacterial inactivation. As such, we can conclude that the mode of action against the targets in WW is a function of the characteristics of the respective addition.

Furthermore, since the study of the regrowth required the dark storage of the samples during the post-treatment period, the MP degradation after 24 h was also performed. In overall, an increment of extra MP degradation was achieved, hence, the process continues in the dark, albeit in lower rates (SM 7). This effect could implies important implications concerning the treatment of WW effluents e.g. in ponds, as the beneficial actions of the (dark) Fenton process continue to be obtained in absence of sunlight.

On the other hand, for wastewater treatment it becomes necessary to evaluate the overall performance of the process. Therefore, the removal of the chemical oxygen demand (COD) and the total

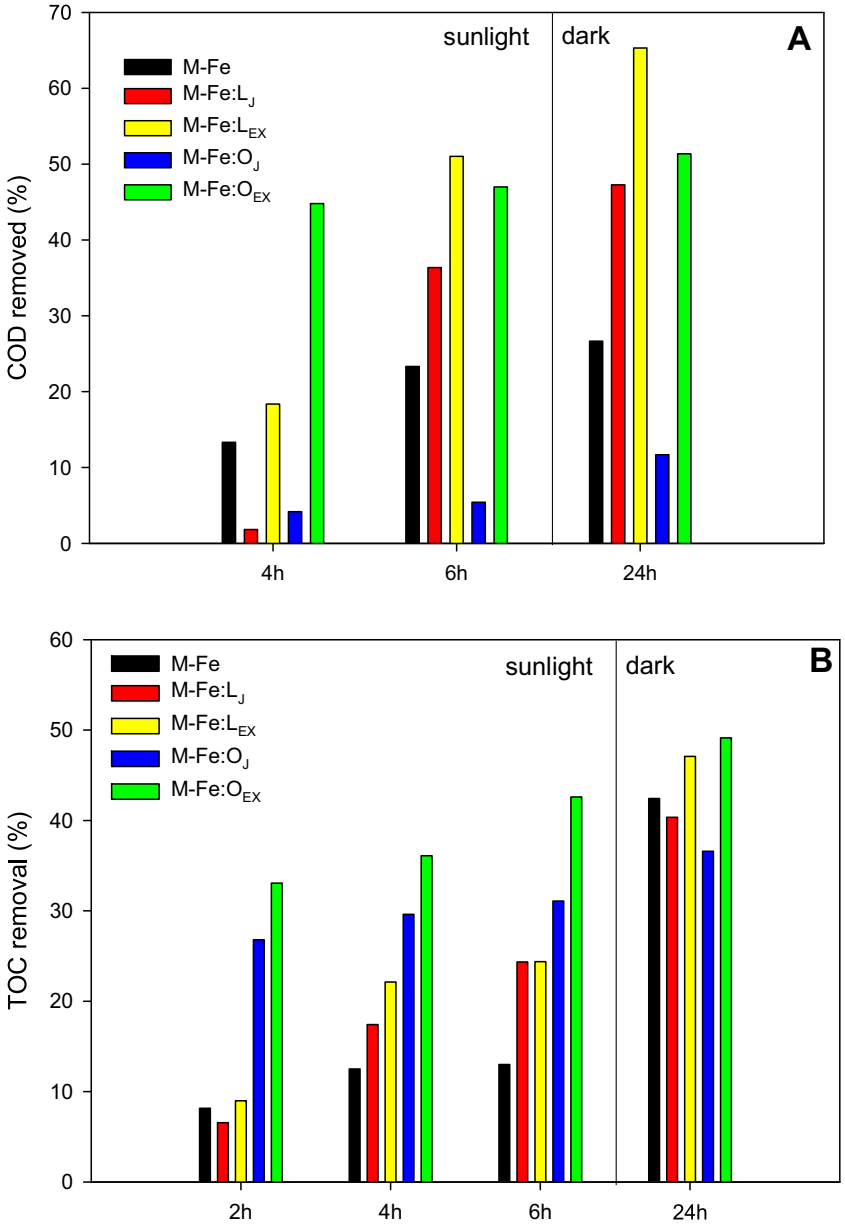

Fig. 8. A) COD removal; B) TOC removal of the secondary effluents treated by solar photo-Fenton using a natural iron material (M-Fe) in the presence natural products: lime juice (L_J) and aqueous extraction (L_{EX}); orange juice (O_J) and aqueous extraction (O_{EX}). [M-Fe] = 5 ppm; [H_2O_2] = 25 ppm; 600 W/m^2. (For interpretation of the references to colour in this figure legend, the reader is referred to the web version of this article.)

organic carbon (TOC) were determined along the treatment giving information of the faith of the organic matter (Fig. 8). For both COD and TOC, an enhancement of the removal by the addition of the natural products can be noticed. In fact, 35% to 50% of COD was eliminated for the lime-based additives and the orange extraction (Fig. 8A). Initial and final (24 h after treatment) values of both COD and TOC are shown in SM 8. A similar tendency was observed for the mineralization level, in which almost 45% of TOC was removed after 6 h of treatment for orange extraction (Fig. 8B). An exception of the enhanced effect of the natural additives was observed for the orange juice case, which has almost no variation for neither the COD nor the TOC, the enhanced solar photo-Fenton treatment. The detrimental effect of the orange juice could be safely attributed to the high concentration of organic matter by its addition. Extra organic matter will subsequently require extra ROS to promote its elimination. Finally, an interesting fact was observed, concerning the increment in COD and TOC removal during the 24-h post-treatment period. In fact, a high mineralization level (almost 50%) was reached in all the systems, including the sole iron material after 24 h, corroborating the previously discussed fact relating to the classic Fenton reaction, still ongoing in the bulk.

4. Conclusions

In this investigation, a new, green way of enhancing the solar photo-Fenton process was evidenced, involving a natural iron source, as iron precursor of the process and natural products as efficient ligands which promote the disinfection capacity of the photo-Fenton process. The use of the natural material leads to several phenomena, involving the production of different reactive species, especially the hydroxyl radical. The efficiency of the process concerning bacterial inactivation was significantly enhanced by the addition of natural products, rich in low weight organic acids: citric, tartaric and ascorbic acid. The addition of caffeic acid as addi-

tive did not show an effect on the bacterial inactivation comparing to the system without enhancement.

This new proposed green process with the natural iron material, enhanced with lime and orange-based additives was efficiently tested for secondary effluents from a municipal treatment plant, reaching total *E. coli* inactivation after the treatment. Moreover, no bacterial regrowth was observed for the most promising systems, i.e. lime-based additives. Additionally, the process promotes a 30% to 40% elimination of the total micropollutants load in wastewater. Consequently, this green process was able to remove 50% of the COD, and reached 40% of mineralization of the EfOM of the bulk (TOC removal) depending on the additive. It must be noted, that contrary to the bacterial elimination, micropollutant degradation was enhanced in similar levels (max 6% difference) among the 4 additions of natural products, hence the utilization of any of the above will enhance MP degradation in the effluents.

All things considered, this investigation suggests a promising way to perform the solar photo-Fenton, as an efficient solution for the treatment of wastewaters contaminated with both bacteria and micropollutants. The use of natural products as precursor of the Fenton process and the enhancement of natural additives show the viability of this process to be applied in developing countries context, by valorizing materials that are otherwise considered as wastes.

Acknowledgments

The authors would like to thank the Swiss Agency for Development and Cooperation (SDC) and the Swiss National Science Foundation (SNSF) through the project “Treatment of the hospital wastewaters in Cote d’Ivoire and in Colombia by advanced oxidation processes”, Project No. 146919. We also thank Margaux Voumard and Christian Pinilla for their contribution, and Soheil Hasanzadeh for the HR-TEM measurements.

Appendix A. Supplementary data

Supplementary data associated with this article can be found, in the online version, at http://dx.doi.org/10.1016/j.apcatb.2017.07.066.

References

[1] N. De la Cruz, L. Esquius, D. Grandjean, a Magnet, a Tungler, L.F. de Alencastro, et al., Degradation of emergent contaminants by UV, UV/H2O2 and neutral photo-Fenton at pilot scale in a domestic wastewater treatment plant, Water Res. 47 (2013) 5836–5845, http://dx.doi.org/10.1016/j.watres.2013.07.005.

[2] S. Giannakis, M.I. Polo, D. López, J.A. Spuhler, P. Sánchez Pérez, C. Fernández Ibáñez, Pulgarón, Solar disinfection is an augmentable, in situ-generated photo-Fenton reactioná—Part 1: a review of the mechanisms and the fundamental aspects of the process, Appl. Catal. B Environ. 199 (2016) 199–223, http://dx.doi.org/10.1016/j.apcatb.2016.06.009.

[3] S. Giannakis, M. Voumard, D. Grandjean, A. Magnet, L.F. De Alencastro, C. Pulgarin, Micropollutant degradation, bacterial inactivation and regrowth risk in wastewater effluents: influence of the secondary (pre)treatment on the efficiency of advanced oxidation processes, Water Res. 102 (2016) 505–515, http://dx.doi.org/10.1016/j.watres.2016.06.066.

[4] S. Miralles-Cuevas, I. Oller, A. Agüera, J.A. Sánchez Pérez, S. Malato, Strategies for reducing cost by using solar photo-Fenton treatment combined with nanofiltration to remove microcontaminants in real municipal effluents: toxicity and economic assessment, Chem. Eng. J. (2016), http://dx.doi.org/10.1016/j.cej.2016.06.031.

[5] S. Arzate, J.L. García Sánchez, P. Soriano-Molina, J.L. Casas López, M.C. Campos-Mañas, A. Agüera, et al., Effect of residence time on micropollutant removal in WWTP secondary effluents by continuous solar photo-Fenton process in raceway pond reactors, Chem. Eng. J. (2017), http://dx.doi.org/10.1016/j.cej.2017.01.089.

[6] S. Giannakis, M.I. Polo López, D. Spuhler, J.A. Sánchez Pérez, P. Fernández Ibáñez, C. Pulgarín, Solar disinfection is an augmentable, in situ-generated photo-Fenton reactionóPart 2: a review of the applications for drinking water and wastewater disinfection, Appl. Catal. B Environ. 198 (2016) 431–446, http://dx.doi.org/10.1016/j.apcatb.2016.06.007.

[7] J.J. Pignatello, E. Oliveros, A. MacKay, Advanced oxidation processes for organic contaminant destruction based on the fenton reaction and related chemistry, Crit. Rev. Environ. Sci. Technol. 36 (2006) 1–84, http://dx.doi.org/10.1080/10643380500326564.

[8] L. Clarizia, D. Russo, I. Di Somma, R. Marotta, R. Andreozzi, Homogeneous photo-Fenton processes at near neutral pH: a review, Appl. Catal. B Environ. 209 (2017) 358–371, http://dx.doi.org/10.1016/j.apcatb.2017.03.011.

[9] S. Papoutsakis, S. Miralles-Cuevas, I. Oller, J.L. Garcia Sanchez, C. Pulgarin, S. Malato, Microcontaminant degradation in municipal wastewater treatment plant secondary effluent by EDDS assisted photo-Fenton at near-neutral pH: an experimental design approach, Catal. Today 252 (2015) 61–69, http://dx.doi.org/10.1016/j.cattod.2015.02.005.

[10] S. Papoutsakis, F.F. Brites-Nóbrega, C. Pulgarin, S. Malato, Benefits and limitations of using Fe(III)- EDDS for the treatment of highly contaminated water at near-neutral pH, J. Photochem. Photobiol. A Chem. 303-304 (2015) 1–7, http://dx.doi.org/10.1016/j.jphotochem.2015.01.013.

[11] N. Klamerth, S. Malato, A. Agüera, A. Fernández-Alba, Photo-Fenton and modified photo-Fenton at neutral pH for the treatment of emerging contaminants in wastewater treatment plant effluents: a comparison, Water Res. 47 (2013) 833–840, http://dx.doi.org/10.1016/j.watres.2012.11.008.

[12] X. Feng, Z. Wang, Y. Chen, T. Tao, F. Wu, Y. Zuo, Effect of Fe(III)/citrate concentrations and ratio on the photoproduction of hydroxyl radicals: application on the degradation of diphenhydramine, Ind. Eng. Chem. Res. 51 (2012) 7007–7012, http://dx.doi.org/10.1021/ie300360p.

[13] B.M. Souza, M.W.C. Dezotti, R.a.R. Boaventura, V.J.P. Vilar, Intensification of a solar photo-Fenton reaction at near neutral pH with ferrioxalate complexes: a case study on diclofenac removal from aqueous solutions, Chem. Eng. J. 256 (2014) 448–457, http://dx.doi.org/10.1016/j.cej.2014.06.111.

[14] D. Spuhler, J. Andrés Rengifo-Herrera, C. Pulgarin, The effect of Fe2+, Fe3+, H2O2 and the photo-Fenton reagent at near neutral pH on the solar disinfection (SODIS) at low temperatures of water containing Escherichia coli K12, Appl. Catal. B Environ. 96 (2010) 126–141, http://dx.doi.org/10.1016/j.apcatb.2010.02.010.

[15] N. De la Cruz, J. Giménez, S. Esplugas, D. Grandjean, L.F. de Alencastro, C. Pulgarín, Degradation of 32 emergent contaminants by UV and neutral photo-fenton in domestic wastewater effluent previously treated by activated sludge, Water Res. 46 (2012) 1947–1957, http://dx.doi.org/10.1016/j.watres.2012.01.014.

[16] A. De Luca, R.F. Dantas, S. Esplugas, Assessment of iron chelates efficiency forphoto-Fenton at neutral pH, Water Res. 61 (2014) 232–242, http://dx.doi.org/10.1016/j.watres.2014.05.033.

[17] S.P. Sun, X. Zeng, A.T. Lemley, Kinetics and mechanism of carbamazepine degradation by a modified Fenton-like reaction with ferric-nitrilotriacetate complexes, J. Hazard. Mater. 252-253 (2013) 155–165, http://dx.doi.org/10.1016/j.jhazmat.2013.02.045.

[18] M.E.T. Sillanpää, T.A. Kurniawan, W. Lo, Degradation of chelating agents in aqueous solution using advanced oxidation process (AOP), Chemosphere 83 (2011) 1443–1460, http://dx.doi.org/10.1016/j.chemosphere.2011.01.007.

[19] P. Villegas-Guzman, S. Giannakis, R.A. Torres-Palma, C. Pulgarin, Remarkable enhancement of bacterial inactivation in wastewater through promotion of solar photo-Fenton at near-neutral pH by natural organic acids, Appl. Catal. B Environ. 205 (2017) 219–227, http://dx.doi.org/10.1016/j.apcatb.2016.12.021.

[20] H. Mechakra, T. Sehili, M.A. Kribeche, A.A. Ayachi, S. Rossignol, C. George, Use of natural iron oxide as heterogeneous catalyst in photo-Fenton-like oxidation of chlorophenylurea herbicide in aqueous solution: reaction monitoring and degradation pathways, J. Photochem. Photobiol. A: Chem. 317 (2016) 140–150, http://dx.doi.org/10.1016/j.jphotochem.2015.11.019.

[21] F.F. Dias, A.A.S. Oliveira, A.P. Arcanjo, F.C.C. Moura, J.G.A. Pacheco, Environmental Residue-based iron catalyst for the degradation of textile dye via heterogeneous photo-Fenton, Appl. Catal. B Environ. 186 (2016) 136–142.

[22] L.G. Devi, M. Srinivas, M.L. ArunaKumari, Heterogeneous advanced photo-Fenton process using peroxymonosulfate and peroxydisulfate in presence of zero valent metallic iron: a comparative study with hydrogen peroxide photo-Fenton process, J. Water Process Eng. 13 (2016) 117–126, http://dx.doi.org/10.1016/j.jwpe.2016.08.004.

[23] F. Chai, K. Li, C. Song, X. Guo, Synthesis of magnetic porous Fe3O4/C/Cu2O composite as an excellent photo-Fenton catalyst under neutral condition, J. Colloid Interface Sci. 475 (2016) 119–125, http://dx.doi.org/10.1016/j.jcis.2016.04.047.

[24] P.T. Almazán-Sánchez, M.J. Solache-Ríos, I. Linares-Hernández, V. Martínez-Miranda, Adsorption-regeneration by heterogeneous Fenton process using modified carbon and clay materials for removal of indigo blue, Environ. Technol. 37 (2016) 1843–1856, http://dx.doi.org/10.1080/09593330.2015.1133718.

[25] M. Usman, P. Faure, C. Ruby, K. Hanna, Remediation of PAH-contaminated soils by magnetite catalyzed Fenton-like oxidation, Appl. Catal. B Environ. 117 (2012) 10–17, http://dx.doi.org/10.1016/j.apcatb.2012.01.007.

[26] S. Muthukumaran, D.A. Nguyen, K. Baskaran, Performance evaluation of different ultrafiltration membranes for the reclamation and reuse of secondary effluent, Desalination 279 (2011) 383–389, http://dx.doi.org/10.1016/j.desal.2011.06.040.

[27] S. Giannakis, E. Darakas, A. Escalas-Cañellas, C. Pulgarin, Elucidating bacterial regrowth: effect of disinfection conditions in dark storage of solar treated secondary effluent, J. Photochem. Photobiol. A Chem. 290 (2014) 43–53, http://dx.doi.org/10.1016/j.jphotochem.2014.05.016.

[28] S. Giannakis, E. Darakas, A. Escalas-Cañellas, C. Pulgarin, The antagonistic and synergistic effects of temperature during solar disinfection of synthetic secondary effluent, J. Photochem. Photobiol. A Chem. 280 (2014) 14–26, http://dx.doi.org/10.1016/j.jphotochem.2014.02.003.
[29] C. Ruales-Lonfat, J.F. Barona, A. Sienkiewicz, J. Vélez, L.N. Benítez, C. Pulgarín, Bacterial inactivation with iron citrate complex: a new source of dissolved iron in solar photo-Fenton process at near-neutral and alkaline pH, Appl. Catal. B Environ. 180 (2016) 379–390, http://dx.doi.org/10.1016/j.apcatb.2015.06.030.
[30] S. Giannakis, F.A. Gamarra Vives, D. Grandjean, A. Magnet, L.F. De Alencastro, C. Pulgarin, Effect of advanced oxidation processes on the micropollutants and the effluent organic matter contained in municipal wastewater previously treated by three different secondary methods, Water Res. 84 (2015) 295–306, http://dx.doi.org/10.1016/j.watres.2015.07.030.
[31] C. Ruales-Lonfat, J.F. Barona, a. Sienkiewicz, M. Bensimon, J. Vélez-Colmenares, N. Benítez, et al., Iron oxides semiconductors are efficients for solar water disinfection: a comparison with photo-Fenton processes at neutral pH, Appl. Catal. B Environ. 166–167 (2015) 497–508, http://dx.doi.org/10.1016/j.apcatb.2014.12.007.
[32] L. Wang, C. Zhang, H. Mestankova, F. Wu, N. Deng, G. Pan, et al., Photoinduced degradation of 2, 4-dichlorophenol in water: influence of various Fe(III) carboxylates, Photochem. Photobiol. Sci. 8 (2009) 1059–1065, http://dx.doi.org/10.1039/b902607j.
[33] B. Song, G. Wang, J. Yuan, Measurement and characterization of singlet oxygen production in copper ion-catalyzed aerobic oxidation of ascorbic acid, Talanta 72 (2007) 231–236, http://dx.doi.org/10.1016/j.talanta.2006.10.021.
[34] J. Bolobajev, M. Trapido, A. Goi, Improvement in iron activation ability of alachlor Fenton-like oxidation by ascorbic acid, Chem. Eng. J. 281 (2015) 566–574, http://dx.doi.org/10.1016/j.cej.2015.06.115.
[35] K. Chvátalová, I. Slaninová, L. Brezinová, J. Slanina, Influence of dietary phenolic acids on redox status of iron: ferrous iron autoxidation and ferric iron reduction, Food Chem. 106 (2008) 650–660, http://dx.doi.org/10.1016/j.foodchem.2007.06.028.
[36] K.L. Penniston, S.Y. Nakada, R.P. Holmes, D.G. Assimos, Quantitative assessment of citric acid in lemon juice, lime juice, and commercially-available fruit juice products, J. Endourol. 22 (2008) 567–570, http://dx.doi.org/10.1089/end.2007.0304.
[37] R.M. Uckoo, G.K. Jayaprakasha, B.S. Patil, Phytochemical analysis of organic and conventionally cultivated Meyer lemons (Citrus meyeri Tan.) during refrigerated storage, J. Food Compos. Anal. 42 (2015) 63–70, http://dx.doi.org/10.1016/j.jfca.2015.01.009.
[38] B.S. Chanukya, M. Prakash, N.K. Rastogi, Extraction of citric acid from fruit juices using supported liquid membrane, J. Food Process Preserv. (2016), http://dx.doi.org/10.1111/jfpp.12790.
[39] R. Scherer, A.C.P. Rybka, C.A. Ballus, A.D. Meinhart, J.T. Filho, H.T. Godoy, Validation of a HPLC method for simultaneous determination of main organic acids in fruits and juices, Food Chem. 135 (2012) 150–154, http://dx.doi.org/10.1016/j.foodchem.2012.03.111.